Ab Initio Studies of the Hydrogen Atom Addition to Ethylene

Okio NOMURA,* and Suehiro IWATA

Institute of Physical and Chemical Research, Hirosawa 2-1, Wakoh, Saitama 351

(Received June 6, 1979)

The ethyl radical formation from hydrogen and ethylene was studied with *ab initio* open shell SCF and CI methods. At first, the minimal basis set (STO-6G) was used to determine a minimal energy path. The calculated exothermicity and the height of the barrier were 72.3 kcal/mol† and 16.9 kcal/mol, respectively. After the full geometry optimization with the double zeta basis set the calculated exothermicity became 38.3 kcal/mol, which is in agreement with the experimental value (40.1 kcal/mol), but the barrier height (16.5 kcal/mol) was no better than that obtained by the minimal basis set. After the extensive CI calculations along Sloane and Hase's path with the minimal basis set, the calculated height of the barrier became only 5.1 kcal/mol. The small but finite barrier height is important in this reaction. The successive hydrogenation to form ethane was also studied and no barrier was found in the reaction.

The addition of hydrogen to ethylene (1),

$$H\cdot + C_2H_4 \rightleftharpoons C_2H_5\cdot^* \longrightarrow C_2H_5\cdot \qquad (1)$$

has long been a concern to chemists as a fundamental model of addition reaction of alkyl to olefins. In recent years several powerful experimental techniques have been developed for studying free radical formation. The analysis of kinetic data clarifies the reaction mechanism and has made activation energy reliable in some important radical reactions within the error of a few kilocalories.[1-4] The experimental activation energy falls between 0.5 and 7 kcal/mol.[1,†] Sato and his collaborators[5] observed the isotopic effect and they suggested that there is a barrier, however small it might be. The exothermicity of the reaction is obtained experimentally as 40.1 kcal/mol,[6] which is equal to the theoretical value obtained by Lathan *et al.*[7] This agreement may be fortuitous, though the heat of formation is not difficult to estimate in the SCF (self-consistent field) calculation as demonstrated by Pople.[8] It is, however, difficult to evaluate the barrier height of radical reactions in which a bonded pair and an unshared electron are exchanged between reactants and products,[9] such as

$$A\text{-}B + C\cdot \longrightarrow A\cdot + B\text{-}C. \qquad (2)$$

The hydrogen exchange reaction H_2+H[10] and the reactions of hydrogen and fluorine, such as $H+F_2$, $H+HF$, and $F+H_2$[11] are among examples for which the barrier height is successfully evaluated by very extensive *ab initio* CI calculations. Another reaction studied theoretically is $H+N_2$,[12] in which three atoms are found not to lie on a line. In this case change of hybridization in the course of reaction plays a significant role.

A more complicated reaction may be an addition of hydrogen (H*) to ethylene. This can be regarded as a model of radical reaction of conjugated hydrocarbons. The reaction has characteristics in change of geometry as well as of hybridization along the reaction path. Bending the CH_2 moiety off the molecular plane is expected to be one of the most important changes in geometry to form a methyl moiety. The transfer of an unpaired electron occurs from the attacking hydrogen to the other side of carbon to which the hydrogen is not attached. Shih *et al.*[13] studied the reaction of $NH_2+C_2H_4$ from a similar point of view. The UHF method might be a convenient tool in discussing the reaction mechanism because it, in many cases, predicts proper dissociation products of a ground state in a single determinant approach at the cost of vitiating the spin symmetry. Sloane and Hase[14a] calculated the potential surfaces of the Reaction 1 using the UHF method with STO-3G and 4-31G. Though geometry optimization was made at each point, they could not find a barrier. Since experimentally the barrier is known to exist in the reaction, in the recent paper,[14b] they had to use the "experimental barrier height" (3.5 kcal/mol at r_{CH}*= 2.0 Å) to derive the analytic potential energy surface. On the other hand, Nagase and Kern,[15a] and Kato and Morokuma[15b] found a very small barrier after careful geometry optimization with the 4-31 G UHF calculations. In the present paper the restricted open shell SCF and CI methods are used for the study of the Reaction 1. At first, several model reaction paths are examined to clarify the change of the electronic structure along the path, and then geometrical parameters are optimized. Finally careful CI calculations along the reaction path determined by Sloane and Hase are performed to compare with the UHF results. The barrier is found both in the restricted SCF and in the CI calculations.

Methods

Restricted SCF Method (RHF): The restricted SCF method for open shell (hereafter it is called RHF as traditionally is) used is essentially equivalent to the two-Hamiltonian method by Davidson.[16] The program written by one of the present authors (S. I.) was linked with GAUSSIAN 70 at the University of Rochester. Since it is also capable of solving the three-Hamiltonian method, the program can be applied to an excited singlet state belonging to an irreducible representation different from that of the closed shell ground state configuration. The closed shell SCF of a cation ($[C_2H_4]H^+$) is first solved to obtain an initial set of orbitals for determining the RHF MO of the radical ($[C_2H_4]H\cdot$). The set of doubly occupied orbitals (ϕ_i, $i=1,\cdots,7$) are first determined and then an electron is added to the vacant orbitals (ϕ_8 or ϕ_9) depending on the state of the radical. The matrix equations to be solved at the $(\nu+1)$th

† 1cal=4.184 J.

cycle are

$$G_C^{\nu} b_C^{\nu+1} \equiv \{F_C^{\nu} - (n_O/n_C)(P_O^{\nu} F_O^{\nu} + F_O^{\nu} P_O^{\nu})\} b_C^{\nu+1} = \varepsilon b_C^{\nu+1}, \quad (3)$$

$$(1-P_C^{\nu+1}) F_O^{\nu} (1-P_C^{\nu+1}) b_O^{\nu+1} = \varepsilon b_O^{\nu+1}, \quad (4)$$

where the occupation numbers, n_C and n_O, in this case, are equal to 2 and 1, respectively. Fock matrices F_C^{ν} of a closed shell and F_O^{ν} of an open shell are defined in terms of the ν-th cycle MO's $\{\phi_k^{\nu}\}$ as

$$(F_C^{\nu})_{jk} = \langle \phi_j^{\nu} | h + 2J_C - K_C + 2J_O - K_O | \phi_k^{\nu} \rangle, \quad (5)$$

$$(F_O^{\nu})_{jk} = \langle \phi_j^{\nu} | h + 2J_C - K_C | \phi_k^{\nu} \rangle, \quad (6)$$

respectively, where J_C and K_C, and J_O and K_O are the coulomb and exchange operators of the closed shell and of the open shell orbitals, respectively. The projection operators P_O^{ν} and $P_C^{\nu+1}$ are defined in the present case as

$$P_O^{\nu} = |\phi_s^{\nu}\rangle\langle\phi_s^{\nu}|, \quad P_C^{\nu+1} = \sum_{k=1}^{7} |\phi_k^{\nu+1}\rangle\langle\phi_k^{\nu+1}|. \quad (7)$$

The transformation of the operator F_O in Eq. 4 by the projection operator $(1-P_C)$ implies that the open shell orbital and the virtual orbitals are determined outside the space spanned by the closed shell orbitals. The orbital energies of both the closed shell and the open shell orbitals satisfy Koopmans' theorem. Generally speaking, convergence is slower than in the closed shell SCF procedure. The orbital set after about fifteen cycles is used as a basis for the MRBW and CI calculations; the energy convergence is about 10^{-4} hartree.

MRBW Method: Even for a system which can be satisfactorily described by a single Slater determinant around its stable geometry, several electronic configurations are required for correct description when the geometry changes to a transition state in a reaction path. The CI calculation may be the best way but it is time-consuming. To estimate the characteristics of the potential energy surface, the second order Brillouin-Wigner perturbation with several reference states is used. The essential idea has been proposed by Löwdin[17] by partitioning a full Hamiltonian matrix into reference (R) and its quotient (Q).

$$H_{\text{eff}}(E) = H_{RR} + H_{RQ}(E - H_{QQ})^{-1} H_{QR} \quad (8)$$

A careful choice of a reference space, R, allows us to regard Eq. 8 as the effective Hamiltonian projected onto the space R. By neglecting the off-diagonal elements of H_{QQ}, the effective Hamiltonian reduces to a simple form,

$$H_{\text{eff}}^{\text{MRBW}}(E) = H_{RR} + H_{RQ}(E - E_Q^{\text{diag}})^{-1} H_{QR}, \quad (9)$$

where H_{RR} and H_{RQ} are the Hamiltonian matrix among reference states and between the reference and the quotient states, respectively. E_Q^{diag} is the diagonal element of H_{QQ}. This perturbation expansion may be called the multi-reference Brillouin-Wigner (MRBW), which is equivalent to the B_k method of Gershgorn and Shavitt[18] and to the method proposed by Segal *et al.*[19] Obviously, in MRBW, the choice of the reference CSF's (configuration state function) is important to obtain the approximate results to the large CI calculation.

CI (Configuration Interaction): A CI program named EFCI[20] consists of six modules as follows.

Link 1. Reading a symmetry table of MO and transforming integrals from AO to MO basis.

Link 2. Generation of electronic configurations. A set of MO's are partitioned into four groups:

i) the fixed core orbitals (which are always doubly occupied),

ii) the core orbitals (hereafter abbreviated as $\{c\}$)

iii) the valence orbitals $\{v\}$, and

iv) the excited orbitals $\{e\}$.

The electronic configurations generated are grouped into nine types. (1) The "valence" CSF: First, all of $\{c\}$ are doubly occupied, and then, the rest of electrons are filled in $\{v\}$. All the possible CSF's are generated without filling electrons in $\{e\}$. The "valence" CSF's are usually the reference states for MRBW and for the configuration selection procedure. The dominant CSF's in the states which are being studied should be included in this type. The other eight types of CSF's are single and double excitations from the "valence" CSF's. (2) $v^2 \rightarrow e^2$ (3) $v \rightarrow e$ (4) $cv \rightarrow e^2$ (5) $c \rightarrow e$ (6) $c^2 \rightarrow e^2$ (7) $c \rightarrow v$ (8) $c^2 \rightarrow ve$ (9) $c^2 \rightarrow v^2$.

Link 3. Evaluation of matrix elements in H_{RR}, H_{RQ} and the diagonal of H_{QQ}, and selection of CSF's in Q using the second-order multi-reference Rayleigh-Schrödinger perturbation expansion (A_k method).[18]

Link 4. Performing MRBW and analysis of the result.

Link 5. Evaluation of off-diagonal matrix elements in H_{QQ}.

Link 6. Solving the eigenvalue problem and analysis of the electron correlation.[21] Davidson's method modified by S. I. is used.[22]

In some cases the type of excitations $c^2 \rightarrow e^2$, though inclusion of this type lowers the total energy considerably, can be neglected because this type of excitations contributes only to the pair correlation energy of the core electrons by shifting all the "valence" states almost uniformly.[21] Care should be taken of the choice of valence orbitals and the threshold value of configuration selection. On a similar account the size of CI is also paid attention to. Hereafter the size of CI calculation is denoted as $[M_{\text{root}}/N_R, N_{\text{Qsel}}/N_{\text{Qgen}}]$, where N_R stands for the number of reference CSF's (which consist, in most cases, of the "valence" states) and M_{root} denotes the number of the eigenstates of H_{RR}, which are used for the CSF selection procedure. N_{Qgen} and N_{Qsel} are the numbers of CSF's generated for the Q space and of selected CSF's for the CI calculation, respectively. If the CSF selection procedure is not applied, the CI size is given by $[N_R, N_{\text{Qsel}}]$.

A deliberate choice of valence orbitals is necessary to take into account a well-balanced correlation along the reaction path. Those orbitals (frontier orbitals) which play an important role in a bond formation or bond exchange should be taken into account in the valence orbitals $\{v\}$. It is necessary to include the antibonding orbitals which suffer considerable changes in the new bond formation, even if they lie much higher than the lowest vacant orbitals.

Results and Discussion

First the SCF calculations are performed along several model paths with a planar ethylene of fixed geometry as shown in Fig. 1. A hydrogen atom attacks an

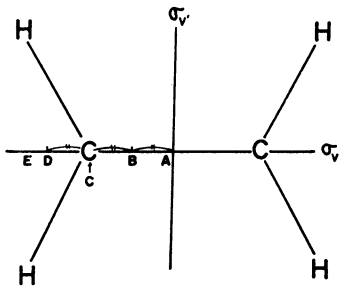

Fig. 1. Attacking points of a hydrogen on the planar ethylene (D_{2h} symmetry) in model calculations. (Only the attack on A has C_{2v} symmetry. Others have C_s symmetry.)

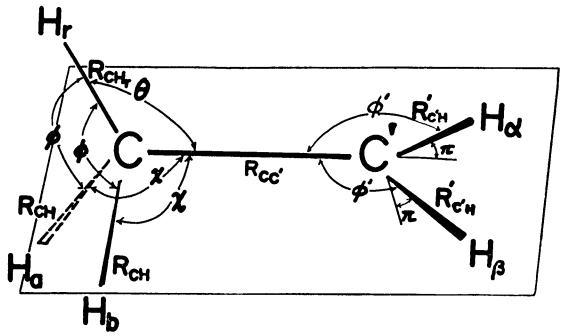

Fig. 2. Parameters of the ethyl for geometry optimization. (C_s symmetry is kept.)

ethylene vertically in the model paths. The vertical approach to the middle point of the C–C bond (path A in Fig. 1) has C_{2v} symmetry. In the paths, B to E, the hydrogen approaches the planar ethylene above the positions shown in Fig. 1. The partial geometry optimization is also performed for these models. These paths are useful for elucidating the origin of the barrier and change of the electron distribution in the course of reaction. Subsequently to the model calculations, the geometrical parameters which are critical to the reaction are optimized. In methyl formation, optimization of the angles ϕ and χ as well as θ defined in Fig. 2 is found to be important. This accounts for the change of hybridization of the carbon atom from sp^2 to sp^3. Sloane and Hase's path[14] is also examined to compare our RHF and CI results with their UHF's. In addition, careful optimization of geometries is made using the RHF method with the double zeta basis set for several important HC_1 distance.

Model A: The potential energy curves for Model A are shown in Fig. 3. In this model the repulsive $^2A_1$ state is dissociated to the ground state ethylene ($^1A_{1g}$) and hydrogen atom (^2S). The other state $^2B_2$ is correlated with the ionic products, $C_2H_4^+(^2B_{1u})+H^-$ in the RHF picture. If the UHF methode is used to describe the dissociation process, this state should be correlated with $C_2H_4(^3B_{2u})+H$. If the C–C bond length, R_{CC} is optimized along with the distance R_{HP} between H and the ethylene plane, the energy is lowered by 18.7 kcal/mol at $R_{HP}=1.1$ Å (see the curve b in Fig. 3). Even after the optimization of R_{CC} the energy minimum of the potential energy curve of $^2B_2$ in model A is found to be higher than the dissociation limit

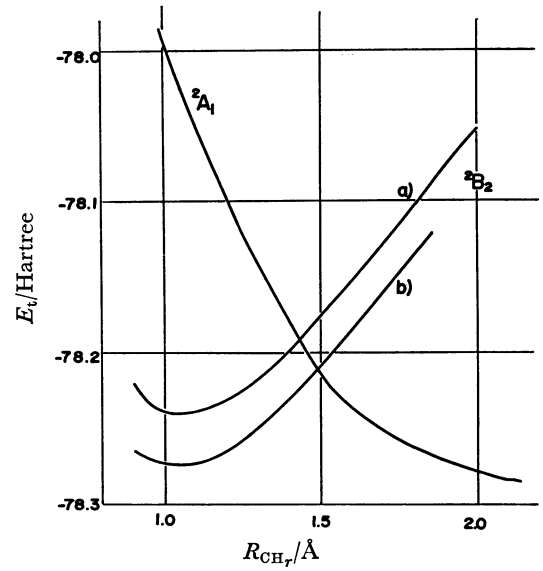

Fig. 3. Potential energy curves of the planar ethyl formation (model A).
a) In $^2B_2$, R_{CC} is fixed at 1.34 Å.
b) In $^2B_2$, R_{CC} is optimized with respect to R_{CH}.

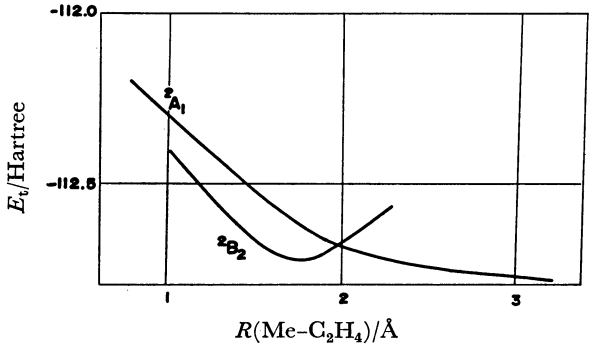

Fig. 4. Potential energy curves of $CH_3+C_2H_4\rightarrow C_3H_7$. Methyl radical approaches the planar ethylene perpendicularly to the middle of the C–C bond. $^2A'$ and $^2A''$ corresponds to the $^2A_1$ and $^2B_2$ in the C_{2v} $H+C_2H_4$ model system.

of C_2H_4+H. The optimization of the out-of-plane angles of CH_2 moieties does not change this conclusion. Although an experimental analysis suggests that CF_3 and CH_3 radicals might give rise to bridged adducts with substituted ethylenes,[23] no stable structures are found in bridged form (model A path) in our SCF calculation for $C_2H_4+CH_3$, as is shown in Fig. 4. This type of symmetric insertion is orbital-symmetry forbidden.[24–26]

Model B—E: In these models, because of the lower symmetry, the states $^2A_1$ and $^2B_2$ in model A can interact with each other. Consequently, at longer R_{HP}, the $^2A_1$ character is dominant in the lowest state while the bonding $^2B_2$ becomes a main component at shorter R_{HP}. At an intermediate R_{HP} the character of the lowest state suddenly changes. Around that distance a hump is expected to be found. The calculated potential energy curves are shown in Fig. 5. In models C, D, and E, C_2H_5 is more stable than the dissociation limit, C_2H_4+H. Among them, the most plausible path of the hydrogen to the planar ethylene is the

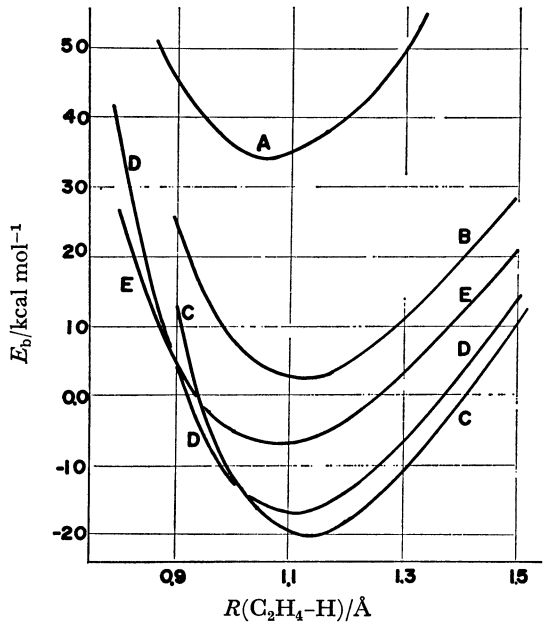

Fig. 5. Potential energy curves of $H+C_2H_4 \rightarrow C_2H_5$ model system (*cf.* Fig. 1). The energy is relative to the dissociation limit.

attack from above a carbon atom (path C). When a hydrogen atom attacks one of the carbon atom C_1, while a new H–C bond is formed, the C–C π bond breaks and an unpaired electron is localized at the other side of carbon C_2. The most stable R_{HC_1} is 1.15 Å; it is a little longer than a usual C–H bond length. As is expected, the hump is found at $R_{HC_1} \approx 1.8$ Å and its height is 20 kcal/mol, which is about several times larger than the experimentally estimated activation energy (see below).

Geometry Optimization: First, three geometry parameters (R_{CC}, θ, and χ) are optimized for each R_{HC_1} along the path C, using STO-6G and open shell RHF; the results are given in Table 1. It is notable that the C–C double bond is suddenly lengthened to become a single bond at the vicinity of the hump of the potential curve. As is mentioned above, at these R_{HC_1}, the main character of the ground state has changed. A similar feature is reported for R_{CN} in the reaction $C_2H_4+NH_2$.[13] Full geometry optimization is carried out using the double zeta basis set and the open shell RHF method at the bottom ($R_{HC_1}=1.1$ Å) and the hump (1.8 Å) determined above by the minimum basis set RHF calculations. The results are given in

Table 1. Optimized geometries
$C_2H_4 + H \rightarrow C_2H_5$ Case C

R/Å	R(C-C)/Å	θ/°	χ/°	E_T/a.u.
0.8	1.512	108.5	110.5	−78.29816
1.0	1.516	109.5	109.3	−78.40805
1.1	1.515	108.8	110.2	−78.41495
1.3	1.505	108.2	110.6	−78.38732
1.5	1.495	105.2	108.8	−78.33173
1.65	1.487	106.0	111.8	−78.29389
1.8	1.365	93.1	118.4	−78.27281
3.0	1.308	89.5	120.2	−78.29760

Table 2. Geometry of the ethyl radical

Parameter[a]	Ours	NK[b]	PD[c]	LHP[d]
R_{HC_1}/Å	1.1	1.089	1.090	1.09
$R_{C_1C_2}$/Å	1.511	1.496	1.498	1.516
$R_{C_1H_a}$/Å	1.094	1.084	1.086	1.087
$R_{C_2H_\alpha}$/Å	1.085	1.073	1.076	1.083
θ/°	111.0	111.7	112.01	111.2
χ/°	110.5	111.4	111.42	110.4
π/°	4.8	8.4	6.19	22.9
ϕ/°	108.0	107.1	—	107.8
ϕ'/°	121.1	120.7	120.6	118.9

a) See Fig. 2 as to the parameter. b) Ref. 29. c) Ref. 27. d) Ref. 7.

Table 3. Geometry of the ethyl at transition state

Parameter[a]	Ours	NK[b]
R_{CH}/Å	1.80	2.015
R_{CC}/Å	1.480	1.357
$R_{C_1H_a}$/Å	1.109	1.072
$R_{C_2H_\alpha}$/Å	1.088	1.072
θ/°	111.2	106.2
ϕ/°	104.8	93.0
χ/°	108.6	121.4
ϕ'/°	120.0	121.6
π/°	10.8	1.9

a) See Fig. 2 as to the parameter. b) Ref. 29.

Tables 2 and 3, and are compared with parameters determined by other workers. The angle π in Fig. 2 is the bending angle of nonreacting CH_2 moiety off the ethylene plane. The geometry of free ethylene with the same basis set is determined as $R_{CC}=1.342$ Å, $R_{CH}=1.084$ Å and $\angle CCH=121.7°$. Previously, Pacansky and Dupuis (PD),[27] Lathan *et al.* (LHP),[7] and Nagase and Kern (NK)[15a] optimized the structure parameters of the ethyl radical C_2H_5. PD used the triple zeta basis set for the RHF calculation and a larger set with polarization functions for the UHF calculation. They found no appreciable difference in the RHF and UHF structures. NK and LHP employed the 4-31G and STO-3G set, respectively and both used UHF method. Agreement between our parameter set and theirs is rather good except for the out-of-plane angle, π, for the $C_2H_\alpha H_\beta$, which is much smaller (4.8°) in ours, then increases in PD's and NK's, and is the largest in LHP's (22.9 °).

The exothermicity calculated by RHF with STO-6G is 72.3 kcal/mol; too large in comparison with the experimental value, 40±1 kcal/mol. The UHF method also overestimates the exothermicity (59.1 kcal/mol by Lathan *et al.*[7] and 76.1 kcal/mol by Sloane and Hase,[14a] if the minimal basis set is used. The use of the double zeta basis set improves this value substantially, which is 38.3 kcal/mol in our calculation and 40.1 kcal/mol in 4-31G UHF calculation by LHP and NK.

The calculated hump height is 12.76 kcal/mol at $R_{CH_1}=1.8$ Å for the STO-6G set and 16.5 kcal/mol at

the same bond length for the double zeta basis set, when the RHF method is applied. On the other hand, Sloane and Hase reported that they found no hump in their UHF potential energy curve.[14a] Very recently Kato and Morokuma,[15b] also using the UHF method and the 4-31G set, optimized the structure of C_2H_5 along the reaction path and found the hump with 2 kcal/mol at R_{HC_1}=2.1 Å, while NK obtained the same barrier at 2.015 Å.[15a] Experimentally, it has been known that the barrier exists in the reaction. Although the experimental activation energies reviewed by Teng *et al.*[1] are scattered from 7.2 to 0.5 kcal/mol, the most probable value may be *ca.* 3 kcal/mol. Our calculated heights are considerably higher than the experimental activation energy. Difficulty in calculating the hump height by RHF is not surprising, because the single electron configuration description such as RHF should fail at the hump region as model calculations (A—E) indicate. To obtain more reliable calculated hump height, the CI calculation is required.

CI Calculations: To compare Sloan and Hase (SH)'s UHF results, the CI calculations are performed along the reaction path determined by SH. The various schemes of the generation of the CSF list are examined. In this series of CI calculations, the STO-6G set is used. The molecular orbitals used are the open shell RHF MO's for the lowest state of ethyl radical. To test the MO set dependence, the closed shell SCF MO's for $C_2H_5^+$ are also used. The convergence is faster in the open shell MO-CI than in the closed shell MO-CI. Below, only the former results are discussed.

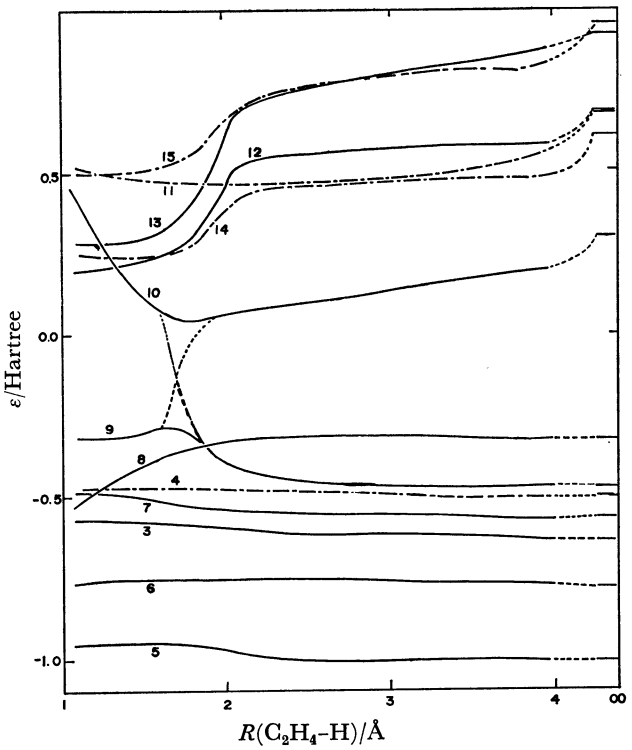

Fig. 6. Orbital correlation diagram for $H+C_2H_4 \rightarrow C_2H_5$ (STO-6G RHF ground state), along the Sloane and Hase's path. Broken lines are for a″ and solid lines for a′.

To obtain even qualitatively correct potential energy surfaces in the CI calculations, it is very important how to generate the SCF list. In our terminology defined in the previous section, the CI results are dependent on the division of the set of MO's into $\{c\}$, $\{v\}$, and $\{e\}$. In Fig. 6 the change of the orbital energies is shown along the path. Note that the number given to each orbital is not the order of the orbital energy. For $R>1.9$ Å, the half filled orbital is the orbital 8, while at $R<1.9$ Å it switches to the orbital 9. Furthermore the character of the orbital 9 changes around the hump; at the shorter distance, the half filled orbital 9 becomes a localized π orbital on C_2. It is worth emphasizing the necessity of drawing the orbital correlation diagram before CI calculations for the potential energy surface. The MO coefficients in Table 4 show change of charracter of the frontier orbitals (ϕ_8, ϕ_9, and ϕ_{10}) as the hydrogen approaches. At R_{HC_1}=4.079 Å, the orbitals ϕ_8 and ϕ_{10} are the bonding and antibonding π of C_2H_4, and ϕ_9 is hydrogen ls. Just after the hump (R_{HC_1}=1.7 Å), where the bond formation between the hydrogen and the C_1 is almost completed, the half filled orbital ϕ_9 becomes localized on the 2pπ lobe of the carbon C_2. The bonding π character of ϕ_8 disappears and the orbital becomes the H–C_1 bonding character. This is also reflected in the H–C_1 antibonding character in ϕ_{10}.

In PCI-1, ECI, and LCI shown in Table 5, the orbitals, 8, 9, and 10 are chosen as the "valence" orbitals, $\{v\}$, and the other occupied and vacant

Table 4. Frontier Orbitals of ethyl radical (Open shell SCF STO-6G)

R(H-C_1)		1.079 Å		
MO		7	9(half)	10
C_1	2pπ	0.5709	−0.0520	1.1178
	2pσ	0.0121	0.0001	0.0247
C_2	2pπ	0.0723	0.9987	−0.1704
	2pσ	−0.0112	−0.0004	−0.0288
H*		−0.4845	0.1703	1.0118
H(C_1)		0.2390	−0.0847	−0.4821
R(H-C_1)		1.700 Å		
MO		8	9(half)	10
C_1	2pπ	0.5739	0.0293	0.8244
	2pσ	0.1041	−0.0034	0.1327
C_2	2pπ	0.1936	−0.9439	−0.3281
	2pσ	−0.0775	−0.0118	−0.3429
H*		−0.6004	−0.3815	0.7754
H(C_1)		0.0954	0.0793	−0.0040
R(H-C_1)		4.079 Å		
MO		8	9(half)	10
C_1	2pπ	0.6314	−0.0043	0.8179
	2pσ	−0.0000	−0.0006	−0.0036
C_2	2pπ	0.6324	−0.0052	−0.8171
	2pσ	0.0000	0.0000	−0.0052
H*		−0.0042	−1.0000	0.0015
H(C_1)		0.0000	0.0006	0.0115

TABLE 5. THE POTENTIAL ENERGIES OF $H+C_2H_4 \rightarrow C_2H_5$ ALONG THE SLOANE AND HASE'S PATH

	RHF	UHF[a)]	PCI-0	[8, 0] PCI-1	[1/8, 1225/4077] ECI	[8, 4077] LCI	[490, 0] PCI-2	[8, 4099] MRBW
1.079	−73.97	−76.1	−74.08	−51.22	−52.6	−52.14	−40.27	−51.28
1.400	−41.58	−45.0	−41.76	−17.89	−38.13	−28.28	−7.22	−36.14
1.700	12.76	−10.5	1.24	1.36	0.84	2.66	23.21	0.71
2.079	8.19	−2.1	6.16	6.08	4.48	5.15	20.20	3.22
4.079	−1.22	0.0	−1.21	1.04	1.45	1.84	24.98	−0.20
$E(\infty)$	−78.2979	−77.54	−78.2979	−78.3431	−78.3778	−78.4562	−78.3778	−78.3772

a) see Ref. 16.

orbitals in the RHF electron configuration are the "core" $\{c\}$ and "excited" $\{e\}$ orbitals along the reaction path. Eight CSF's are constructed by filling three electrons in three "valence states". In LCI, all possible single and double electron excitations (N_{Qgen}=4077) from the "valence states" are taken into account. In ECI the CSF selection procedure are performed with a threshold value (10^{-4} h). These three CI potential curves agree qualitatively with each other as shown in Table 2, although the total electron energies in three calculations differ substantially. The MRBW calculations reproduce the ECI results except at R_{HC_1}=4.079 Å. There are several differences in the CI and RHF curves. The exothermicity and hump height are improved, and in addition, the hump position moves to a longer R_{HC_1}. Since our basis set used in CI is minimal, the calculated exothermicity (52 kcal/mol) and hump height (5 kcal/mol) may be satisfactorily in good agreement with the experiments. Surprisingly, the very small CI (PCI-1) among 8 CSF's can produce the qualitatively correct potential curve. This is because our choice of the "valence orbitals" are suitable for the potential curve calculations; in this sense, the orbitals, 8, 9, and 10, given in Table 2 can be called the "reaction orbitals".[25)]

Our CI potential curves are differnt even qualitatively from the UHF curve obtained by Sloan and Hase, even though the reaction path is the same. As Yamaguchi[25)] pointed out, the UHF (different orbitals for different spins, DODS) wavefunction for three electron-three orbital model, $|\psi_{1\alpha}\ \psi_{2\alpha}\ \overline{\psi}_{1\beta}|$ can be expanded in terms of four electron configurations, $|\chi_a\overline{\chi}_a\psi_{2\alpha}|$, $|\chi_b\overline{\chi}_b\psi_{2\alpha}|$, $|\chi_a\overline{\chi}_b\psi_{2\alpha}|$, and $|\chi_b\overline{\chi}_a\psi_{2\alpha}|$, where χ_a and χ_b are linear combinations of $\psi_{1\alpha}$ and $\psi_{1\beta}$, but the coefficients of these four Slater determinants are severely restricted in the UHF wavefunction. To compare the UHF results, the 3×3 CI calculations among $|\psi_8\overline{\psi}_8\psi_9|$, $|\psi_{10}\overline{\psi}_{10}\psi_9|$ and $1/\sqrt{2}[|\psi_8\overline{\psi}_{10}\psi_9|+|\psi_{10}\overline{\psi}_8\psi_9|]$ are carried out and the energies are shown as PCI-0 in Table 5. Again, the potential curve behaves correctly. These results clearly show that the CI or MCSCF calculations combined with an appropriate choice of the "reaction orbitals" are suitable for the study of the reaction potential curves. As another example of the importance of a careful selection of the "reaction orbitals", is given the PCI-2 calculations in Table 5, where 490 CSF's are created by filling nine electrons in seven orbitals (3a'—9a'). The potential curve thus obtained is absurd.

Ethane Formation: Addition of hydrogen to ethyl radical is studied to see the feature of the successive hydrogenation of ethylene,

$$C_2H_5 + H \longrightarrow C_2H_6^* \longrightarrow C_2H_6. \quad (9)$$

Two curves are obtained in the SCF calculations. One (b in Fig. 7) is the result by the closed shell RHF which is correlated with the ethane formation. The other (a) is the curve obtained by the open shell RHF which leads to the dissociation product. The latter curve is already flat at the intersection of two curves. This implies that the dissociation is an almost complete at the bond length as short as 2 Å (Fig. 7) and that there may be no activation barrier in the ethane formation. In fact, the potential energy curve (c) obtained by CI shows no barrier. It is in conformity with the experimental facts that the rate of the ethane formation is hundred times as fast as that of the ethyl radical formation and that the abstraction of hydrogen by the ethyl easily occurs.

The MO basis set for CI at shorter C–H distance was obtained by the closed shell SCF. The ground electron configuration is $(1a')^2\cdots(5a')^2(1a'')^2(6a')^2(7a')^2(2a'')^2$. The next important configurations are a pair excitation to an antibonding orbital 8a' from the 7a' orbital with mixed character of C–H and C–C bonding, and the double excitation from 1a''

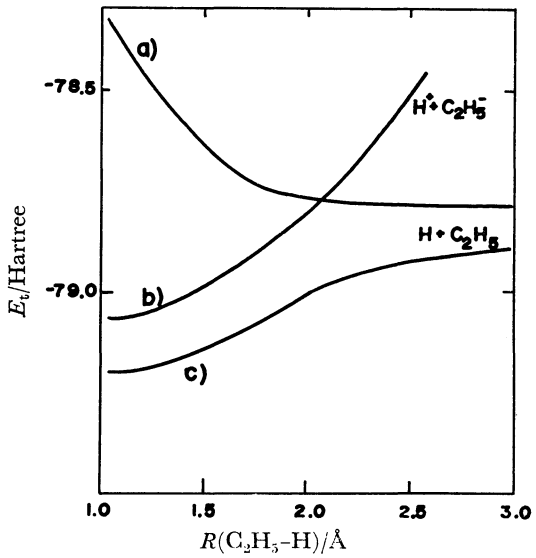

Fig. 7. Potential energy curves of ethane formation. a) Open shell SCF, b) closed shell SCF, c) CI.

and 2a″ to 3a″ and 4a″.These configurations are used as the reference states in the large CI calculation. At $R_{HC_1}=2$ Å the open shell SCF energy is slightly lower than that of the closed shell SCF. The highest occupied MO 7a′ and the lowest vacant MO 8a′ in the closed SCF MO are of the character of C–H bonding and C–H antibonding, respectively. Because of restriction of the double occupancy, the wavefuction is of too strong an ionic character. The open shell SCF makes it possible to localize electronic charge on each atom by a linear transformation of the orbitals. The frontier orbitals obtained by the open shell SCF take the form of hydrogen 1s orbital and unpaired pπ orbital on the carbon. The small energy difference between the two configurations suggests considerable configuration mixing. The CI based on the open shell SCF MO shows that the open shell electronic structure (i) $\Lambda_2(5a')^2(6a')^2(2a'')^2(7a')^1(8a')^1$ is dominant. The complementary ones are composed of closed shell structures (ii) $\Lambda_2(5a')^2(6a')^2(2a'')^2(7a')^2$ and (iii) $\Lambda_2(5a')^2(6a')^2(2a'')^2(8a')^2$, where $\Lambda_2=(1a')^2(2a')^2(3a')^2(4a')^2(1a'')^2$. The wavefunction can be approximated as: $\Psi=0.90$ (i) -0.29 (ii) -0.24 (iii). A linear transformation of the relevant orbitals among the major three configurations reduces to a single configuration wavefunction $\Psi=^1(\phi,\phi)$, with orbitals $\phi=0.97(p\pi)-0.07$ h and $\phi=1.02$ h$-0.05(p\pi)$, where h and pπ denote the hydrogen ls orbital and the unpaired pπ on a carbon, respectively. On the other hand, the half filled orbitals determined by the open shell SCF are of the pure pπ and h character. Further decrease of the interaction between the hydrogen and the carbon changes the orbital character. At $R_{HC_1}=3$ Å the molecule can be regarded as a mixed system composed of a hydrogen atom and an ethyl radical, since 7a′ and 8a′ have characters of pure hydrogen ls orbital and of an unpaired pπ orbital, respectively. The orbital energy of the 7a′ differs no more than 2 kcal/mol from the free hydrogen atom. The predominant configuration is $\Lambda_2(5a')^2(6a')^2(2a'')^2(7a')^1(8a')^1$. The complementary configurations are used to improve the other methyl moiety by promoting one or two electrons in the 6a′ orbital (σ C–H) to the 11a′ (σ^* C–C).

We wish to express our thanks to generous hospitality and suggestions given by Professor Keiji Morokuma and the members in his laboratory at the Institite of Molecular Science in Okazaki. Computation is performed with FACOM 230-75 (Fujitsu Co., Ltd.) in our Institute. Part of the work was supported by the Scientific Grant from Ministry of Education (No. 154144 and 254148).

References

1) W. E. Jones, S. D. Macknight, and L. Teng, *Chem. Rev.*, **73**, 407 (1973).
2) V. V. Voevodskii and V. N. Kondrat'ev, *Progr. React. Kinet.*, **1**, 41 (1961).
3) K. Yang, *J. Am. Chem. Soc.*, **84**, 719 (1962).
4) V. V. Azatyan, A. B. Nalbandyan, and M. Y. Ts'ui, *Dokl. Akad. Nauk SSSR*, **149**, 1095 (1963).
5) Y. Ishikawa, M. Yamabe, A. Noda, and S. Sato, *Bull. Chem. Soc. Jpn.*, **51**, 2488 (1978).
6) J. L. Franklin, J. G. Dillard, H. M. Rosenstock, J. T. Herron, and K. Draxel, NSRDS-NBS-26, National Bureau of Standards (Estimation of the heat of formation is based on the data).
7) W. A. Lathan, W. J. Hehre, and J. A. Pople, *J. Am. Chem. Soc.*, **93**, 808 (1971).
8) "MTP International Review of Scienec," ed by W. B. Brown, Butterworth & Co. London (1972), Vol. 1.
9) "Theoretical Chemistry," ed by R. N. Dixon and C. Thomson, Chem. Soc., London (1975), Vol. 2.
10) B. Liu, *J. Chem. Phys.*, **58**, 1925 (1973).
11) a) C. F. Bender, P. K. Pearson, S. V. O'Neil, and H. F. Schaefer III, *J. Chem. Phys.*, **56**, 4626 (1972); *Science*, **176**, 1412 (1972); b) S. V. O'Neil, P. K. Pearson, H. F. Schaefer III, and C. F. Bender, *J. Chem. Phys.*, **58**, 1126 (1973).
12) K. Vasudevan, S. D. Peyerimhoff, and R. J. Buenker, *J. Mol. Struct.*, **29**, 285 (1975).
13) S. Shih, R. J. Buenker, S. D. Peyerimhoff, and C. J. Michejda, *J. Am. Chem. Soc.*, **94**, 7620 (1972).
14) a) C. C. Sloane and W. L. Hase, *Discuss. Faraday Soc.*, **62**, 210 (1977). In fact, even in their calculation, a very low hump is found, if the energy at the dissociation limit (C_2H_4+H) is correctly evaluated. They took $R_{HC_1}=4.079$ Å as the dissociation limit; b) W. L. Hase, G. Mrowka, R. J. Brudzynski, and C. S. Sloane, *J. Chem. Phys.*, **69**, 3548 (1978).
15) a) S. Nagase and C. W. Kern, *J. Am. Chem. Soc.*, to be appeared. b) S. Kato and K. Morokuma, *J. Chem. Phys.*, in press.
16) E. R. Davidson, *Chem. Phys. Lett.*, **21**, 565 (1973).
17) P.-O. Löwdin, *J. Mol. Spectrosc.*, **10**, 12 (1963); **13**, 326 (1964).
18) Z. Gershgorn and I. Shavitt, *Int. J. Quantum Chem.*, **2**, 751 (1968).
19) G. A. Segal, R. W. Wetmore, and K. Wolf, *Chem. Phys.*, **30**, 269 (1978).
20) Coding of EFCI started when S. I. stayed at University of Chicago. He is grateful to Prof. K. Freed for his support and suggestion.
21) N. Kosugi, H. Kuroda, and S. Iwata, *Chem. Phys.*, **39**, 337 (1979).
22) E. R. Davidson, *J. Comp. Phys.*, **17**, 87 (1975).
23) A. P. Stefani, L-Y. Y. Chuang, and H. E. Todd, *J. Am. Chem. Soc.*, **92**, 4168 (1970).
24) K. Yamaguchi, *Chem. Phys. Lett.*, **28**, 93 (1974).
25) K. Yamaguchi, *Chem. Phys.*, **25**, 215 (1977).
26) V. Bonacic-Koutecky, J. Koutecky, and L. Salem, *J. Am. Chem. Soc.*, **99**, 842 (1977).
27) J. Pacansky and M. Dupuis, *J. Chem. Phys.*, **68**, 4276 (1978).